Contents lists available at ScienceDirect

Electrochimica Acta

journal homepage: www.elsevier.com/locate/electacta

The effect of cobalt on the electrochemical performance of β-nickel hydroxide electrodes

T.N. Ramesh [a,b,*], P. Vishnu Kamath [b]

[a] Department of Inorganic and Physical Chemistry, Indian Institute of Science, Bangalore 560 012, India
[b] Department of Chemistry, Central College, Bangalore University, Bangalore 560 001, India

ARTICLE INFO

Article history:
Received 1 April 2008
Received in revised form 2 June 2008
Accepted 18 June 2008
Available online 27 June 2008

Keywords:
Nickel hydroxide
Cobalt additive
Structural disorder
Stacking faults
Electrochemical activity

ABSTRACT

Crystalline β-nickel hydroxide comprises of a periodic stacking of charge neutral nickel hydroxide layers. Translation or rotation of nickel hydroxide layers with respect to each other generates stacking faults while an intergrowth of one polymorphic modification in the other generates interstratification. These changes generate structural disorder within the sample and the phases are designated as β_{bc} (bc-badly crystalline) nickel hydroxide. The structure, composition and morphology of these phases differ significantly compared to highly ordered crystalline β-nickel hydroxide. Crystalline β-nickel hydroxide exchanges 0.3e/Ni whereas stacking faulted β-nickel hydroxide and β_{bc}-nickel hydroxide exchanges 0.8–0.9e/Ni. Inclusion of cobalt metal as a conducting additive during the electrode fabrication of pasted electrodes is expected to enhance the electrochemical performance of nickel hydroxide. In contrast to the literature reports, partial substitution of cobalt for graphite to highly ordered crystalline phase of β-nickel hydroxide does not show any improvement in their electrochemical activity. Stacking faulted β-nickel hydroxide, β_{bc}-nickel hydroxide and chemically substituted nickel hydroxide samples also does not show any enhancement in their reversible discharge capacity on inclusion of cobalt. This clearly demonstrates that the electrochemical activity is mainly dictated by the structural disorders at 25–30 °C.

1. Introduction

Perfectly ordered crystalline solid comprises of a long range periodic arrangement of atoms. In reality, they often depart from their ideal structure, symmetry, composition and bonding [1]. This deviation from their ideal state is designated by the term disorder [2]. Layered materials are especially prone to disorder as the bonding in select directions is of the weak van der Waal's variety [3]. Prominent among the layered bivalent metal hydroxides is the nickel hydroxide. Nickel hydroxide crystallizes in different polymorphic modifications, i.e. α and β, of which β-phase is widely used as the positive electrode material in all nickel based secondary cells [4]. The oxidation–reduction reaction involves diffusion of protons during the charge–discharge process and can be written as

$$Ni(OH)_2 + OH^- \leftrightarrow NiOOH + H_2O + e^-$$

Bode et al. have reported two redox couples, i.e. β/β couple and α/γ couple β and α for phases of nickel hydroxide [5]. The electrochemical activities of α and β phases of nickel hydroxide differ from one other due to the changes in their structure, composition and morphological features [6]. The presence of water molecules within the interlamellar gallery increases the *d* spacings from 4.6 Å to 7.6 Å in α-nickel hydroxide. Water molecules within the layers of α-nickel hydroxide will also provide a good pathway for the diffusion of protons during the redox process thereby expected to deliver better electrochemical performance [7]. The α-nickel hydroxide being a metastable phase will undergo transformation to thermodynamically stable β-nickel hydroxide in the electrolyte during the charge–discharge process. This hinders the potential utilization of α-phase of nickel hydroxide as an electrode material. During the discharge process, the nickel oxyhydroxide gets reduced to nickel hydroxide. Nickel hydroxide being a wide-band gap semiconductor [8] severely restricts the discharge process by breaking electrical contact between the particles of the active material. Therefore the electrode fabrication plays a crucial role on the electrochemical activity of nickel hydroxide. General factors that can contribute to the electrochemical performance of a working electrode are: (i) the nature of support, (ii) the nature of active material and (iii) conductivity between the support and the active material. The nature of active material and the conductivity factor on the electrochemical performance has been

* Corresponding author. Tel.: +91 80 22961354.
E-mail address: adityaramesh77@yahoo.com (T.N. Ramesh).

0013-4686/$ – see front matter © 2008 Elsevier Ltd. All rights reserved.
doi:10.1016/j.electacta.2008.06.035

examined [7,9,10]. The active material utilization of nickel hydroxide is enhanced when the sample has smaller particle size [11], poor crystallinity [12], high tap density [13] and high moisture content [14]. In addition to the above factors, structural disorders such as stacking faults [15] and compositional disorders such as interstratification and cation vacancies [16] are also known to contribute to higher active material utilization. Inclusion of cobalt as additives in nickel hydroxide is most widely investigated but the exact mechanism is still less understood. Cobalt powder/CoO/$Co(OH)_2$ has been either blended with the active material during electrode preparation or coprecipitated along with nickel hydroxide during the synthesis [17,18]. Electroless deposition of cobalt on nickel hydroxide particles has also been reported [19]. Oshitani et al. [20] and Tarascon and co-workers [21] have extensively studied the effect of cobalt on the electrochemical performance and optimized the conditions to obtain materials which can deliver >1e exchange. There are also reports which discuss about the addition of cobalt to nickel hydroxide electrodes and observe an increase in the conductivity, increase in the oxygen evolution potential, and delay in the mechanical failure of the electrodes [22,23].

Major limitations in most of these studies are (i) the use of commercial grade β-nickel hydroxide in which the exact preparation conditions are not clearly known [24,25], (ii) the active material by default contains small percentage of zinc and cobalt which in principle could have affected the crystal structure as well as the electrochemical activity [19,26] (iii) in certain cases the powder X-diffraction patterns for nickel hydroxide samples are not reported [27–29] and (iv) correlation of particle size with the electrochemical property [30–32]. If we carefully examine the PXRD patterns of the nickel hydroxide which delivers better electrochemical activity even in the presence of cobalt, we observe either (i) broadening of $(h\,0\,\ell)$ reflections [12,17,30] or (ii) broadening of non-$(h\,k\,0)$ reflections.

Does the cobalt addition indeed alter the electrochemical properties of nickel hydroxide, or it merely provides conductivity to the nickel hydroxide/nickel oxyhydroxide matrix. Fierro et al. [33] demonstrate that the addition of cobalt assists to retain the electrochemical performance of nickel hydroxide at 65–80 °C. As a part of our continuing effort to understand the origin of the superior electrochemical activity of high performance nickel hydroxide electrode materials, we examined the effect of (i) cobalt metal powder as a conducting support in place of graphite in the pasted electrodes fabricated from crystalline phase of β-nickel hydroxide, stacking faulted β-nickel hydroxide, β_{bc}-nickel hydroxide, (ii) cobalt substituted crystalline β-nickel hydroxide, β_{bc}-nickel hydroxide samples. The objective of our present study was to examine, whether the addition of cobalt can modify the electrochemical performance of these phases of nickel hydroxide. Crystalline β-nickel hydroxide reversibly exchanges 0.3e/Ni while stacking faulted β-nickel hydroxide and β_{bc}-nickel hydroxide electrodes deliver 0.9e/Ni separately. On substitution of 50 wt% of graphite by cobalt metal as conducting material during electrode fabrication in all these nickel hydroxide samples did not enhance the electrochemical activity. Even cobalt substituted β-nickel hydroxide and β_{bc}-nickel hydroxide samples do not show any dramatic improvement in their electrochemical activity. Therefore we report in this paper that the partial substitution of cobalt in place of graphite or chemical substitution of cobalt into the nickel hydroxide matrix to provide conductivity either by physical or chemical means does not improve the electrochemical activities of β- and β_{bc}-phases of nickel hydroxide. The critical determining factor is the structural disorder present in the sample at ambient conditions (25–30 °C).

2. Experimental

Nickel hydroxide samples were prepared as follows:

(i) By the slow addition of nickel nitrate solution (1 M, 50 mL, 4 mL min^{-1}) to a NaOH (2 M, 100 mL) at 65 °C (pH >13) [12] and the sample is labeled as SH65.
(ii) By the addition of ammonia (2 M, 100 mL, 4 mL min^{-1}) to an aqueous nickel nitrate solution (1 M, 50 mL) at 65 °C (pH ≈10) and the sample is labeled as WH65.

The resultant green slurries were aged for 18 h at 65 °C prior to filtration.

In separate experiments, cobalt substituted nickel hydroxides were obtained by the addition of mixed metal nitrates solution [$(Ni(NO_3)_2$ and $Co(NO_3)_2$] in the mole ratio (0.95:0.05; 0.90:0.1) to NaOH (100 mL, 2 M) at 65 °C (pH >13). The obtained slurry was divided into two parts: one part of the slurry was aged in mother liquor at 65 °C for 18 h to obtain the badly crystalline phase of β_{bc}-nickel hydroxides [labeled as β_{bc}-$Ni_{0.95}Co_{0.05}(OH)_2$; β_{bc}-$Ni_{0.90}Co_{0.10}(OH)_2$] and another part was hydrothermally treated at 170 °C for 18 h in mother liquor (pH >13) (50% filling) to obtain crystalline phases of cobalt substituted nickel hydroxide samples [labeled as β-$Ni_{0.95}Co_{0.05}(OH)_2$].

The precipitates were washed free of alkali and dried at 65 °C till constant weight attained. Commercial nickel hydroxide was obtained from Aldrich (USA) and used as such (labeled as ACC).

All the samples were characterized by PXRD using Siemens D5005 diffractometer with a Cu Kα (λ = 1.5418 Å) source. Data were collected at a scan rate of 4° min^{-1} and rebinned into 2θ steps of 0.05°. Infrared spectra were obtained using a Nicolet Model Impact 400D FTIR spectrometer (KBr pellets, resolution 4 cm^{-1}). Thermogravimetric analysis of all the samples were carried out in air using Mettler Toledo Model 850e TG/SDTA system (heating rate 5 °C min^{-1}). The morphology of the samples was measured using electron microscopy (JEOL JEM 200CX electron microscope 200 kV, holey carbon grids: 200 mesh size). The chemical composition of all the samples were analyzed by wet techniques as described elsewhere [12]. Cobalt content in cobalt substituted nickel hydroxide samples was measured using EDAX analysis (JEOL 200 kV Electron Microscope). All the samples reported here have $[OH^-]/[Ni^{2+}]$ ratio of 2. The unaccounted weight, if any, was attributed to the water content of the samples. The resulting composition was verified

Table 1
Results of wet chemical analysis of the β-nickel hydroxide samples

Sample	Ni^{2+} (wt%)	Co^{2+} (wt%)	OH^- (wt%)	H_2O (wt%)	Approximate formula	Total weight loss (%)†	Reversible moisture content (%)
WH65	61.81	–	35.68	2.52	$Ni(OH)_{2.0}\cdot 0.13H_2O$	20.46 (21.4)	1
SH65	53.39	–	31.10	15.5	$Ni(OH)_{2.0}\cdot 0.9H_2O$	29.3 (32.1)	11
ACC	61.76	–	36.01	2.23	$Ni(OH)_{2.0}\cdot 0.12H_2O$	20.9 (21.4)	2
β_{bc}-$Ni_{0.95}Co_{0.05}(OH)_2$	52.55	2.49	36.76	8.2	$Ni_{0.95}Co_{0.05}(OH)_2\cdot 0.5H_2O$	27.6 (28.2)	11
β_{bc}-$Ni_{0.90}Co_{0.10}(OH)_2$	61.2	7.06	31.76	2	$Ni_{0.90}Co_{0.10}(OH)_2\cdot 0.1H_2O$	27.3 (25.7)	9.5
β-$Ni_{0.95}Co_{0.05}(OH)_2$	58.53	3.16	32.8	5.51	$Ni_{0.95}Co_{0.05}(OH)_2\cdot 0.2H_2O$	2.3 (22.6)	4

† Values in parentheses are calculated on the basis of the approximate formula.

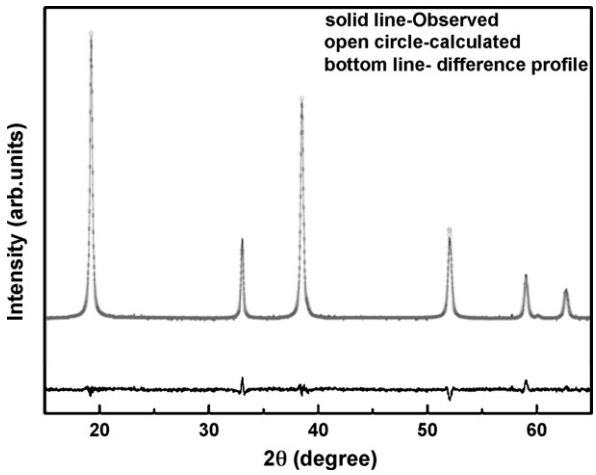

Fig. 1. Rietveld refinement of the structure of WH65 nickel hydroxide.

both by drying studies and thermogravimetric data and found to be consistent (see Table 1).

The electrodes were prepared by mixing active material, graphite powder, and polytetrafluoroethylene suspension (33% suspensions in the weight ratio of 60:30:10 were thoroughly ground to a paste-like consistency to yield control electrodes. To study the effect of cobalt on the electronic conductivity and electrochemical performance, the test electrodes were prepared by replacement of half the graphite (out of 30 wt%) taken by the cobalt metal powder (15 wt%). This was done to maintain the loading levels of the active material constant and facilitate a direct comparison between the control and test electrodes. The paste was pressed onto a nickel foam (2.9 cm × 2.3 cm) at 120 kg cm^{-2} pressure at 25–30 °C. The electrodes were soaked in 6 M KOH for 24 h and galvanostatically charged to 120% of the theoretical capacity. Charge discharge studies were carried out in a half cell. Nickel plate counters were used for cycling and all potentials were measured using a Hg/HgO/OH$^-$ in 6 M KOH. The theoretical capacity corresponds to 1e change. The electrodes were discharged at approximately C/2 rate to a cut-off voltage of 0 V at 28–30 °C. All capacities are normalized to the weight of the active material. Cyclic voltammetric studies were carried out on all the nickel hydroxide samples at different scan rates (10, 20, 40, 60 and 100 mV s^{-1}).

Table 2
Results of the Rietveld refinement of WH65 sample

	Pseudo-Voigt function
Space group	*P*-3*m*1
Cell parameters	
a (Å)	3.1296(6)
c (Å)	4.6147(5)
Shape parameters	
U	0.6019(6)
V	−0.3286(9)
W	0.6019(6)
X	–
Y	–
η(*PV*) or *m*(*P-VII*)	0.7704(3)
z(oxygen)	0.2182(5)
Goodness-of-fit	
R_{wp}	9.59
R_{Bragg}	2.38
R_F	2.21
R_p	10.8
χ^2	1.99

Table 3
Cell dimensions of all the nickel hydroxide samples

Sample	*a* (±0.001 Å)	*c* (±0.001 Å)
WH65	3.12	4.62
ACC	3.12	4.63
SH65	3.12	4.61
β-$Ni_{0.95}Co_{0.05}(OH)_2$	3.13	4.61
β_{bc}-$Ni_{0.95}Co_{0.05}(OH)_2$	3.12	4.61
β_{bc}-$Ni_{0.90}Co_{0.10}(OH)_2$	3.12	4.58

2.1. Structure refinement

Rietveld analysis was carried out on the highly ordered crystalline phase of β-nickel hydroxide (WH65). The cell dimensions and the atomic position coordinates were obtained from the literature for the Rietveld analysis [34].

2.2. PXRD simulation studies

The line shape function and the input parameters used for DIFFaX simulations were obtained from the output of Rietveld refinement of WH65 nickel hydroxide sample. The PXRD patterns were simulated using the DIFFaX code [35] and the details reported elsewhere [36]. The goodness of fit was judged by the difference profile and calculating the reliability factor R_{wp} (%).

3. Results and discussion

The structure, composition and morphological features of β-phases of nickel hydroxides depend on the precipitation conditions. Fig. 1 shows the results of the Rietveld analysis of WH65-nickel hydroxide sample. The refined parameters of WH65 nickel hydroxide with the goodness of fit values are given in Table 2. The atomic position coordinates and the Ni–O bond distance is in close agreement with the values reported by Greaves and Thomas [34]. The goodness of fit values is in the acceptable range considered by Young [37]. The cell parameters of all the nickel hydroxide samples are reported in Table 3. The Scherrer formula was applied to all the reflections in the PXRD patterns and the crystallite sizes were estimated. The estimated crystallite sizes of different nickel hydroxide samples are given in Table 4.

Fig. 2A shows the PXRD patterns of ACC and SH65 nickel hydroxide samples. The prominent reflections in the PXRD pattern of ACC and SH65 nickel hydroxides appear at the similar *d*-spacings to that of WH65 nickel hydroxide. If we examine the chemical composition of WH65 and ACC, they are almost similar, but the PXRD patterns differ from one another due to the broadening of (*h* 0 *ℓ*) reflections. In ACC nickel hydroxide, we observe excessive broadening of the (1 0 2) reflection in addition to the broadening of (0 0 1) reflection. The PXRD pattern of SH65 (see Fig. 2B) display peaks corresponding to non-(*h k* 0) reflections are considerably broadened compared to the reflections in the PXRD pattern of WH65 nickel hydroxide given in Fig. 1. This clearly shows the poor crystalline nature of SH65 nickel hydroxide. During the transformation from α-phase

Table 4
Estimated crystallite sizes (±0.4 Å) based on the width of all the reflections in the PXRD patterns of nickel hydroxide samples

Sample	(0 0 1) (Å)	(1 0 0) (Å)	(1 0 1) (Å)	(1 0 2) (Å)	(1 1 0) (Å)	(1 1 1) (Å)
SH65	28	173	35	–	431	215
ACC	187	633	135	68	516	434
WH65	702	1054	677	718	1030	913
β_{bc}-$Co_{0.05}$	29	183	45	–	228	172
β_{bc}-$Co_{0.10}$	69	226	49	–	310	96
β-$Co_{0.05}$	526	474	328	392	813	413

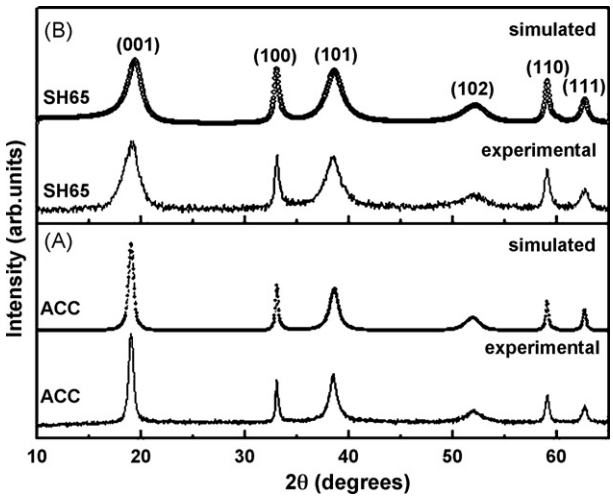

Fig. 2. Comparison of an (A) observed and the simulated PXRD patterns of ACC nickel hydroxide and (B) observed and the simulated PXRD patterns of SH65 nickel hydroxide (solid line is observed and open circles are the simulated PXRD patterns).

of nickel hydroxide to highly crystalline β-phase of nickel hydroxide there occurs phases with an intergrowth of α-phase of nickel hydroxide within the β-phase thereby affecting the crystallinity of the sample. Intergrowth of a small percentage α-nickel hydroxide within the β-phase is referred to as β_{bc}-nickel hydroxide (bc: badly crystalline).

The non-uniform broadening of lines in the PXRD pattern of nickel hydroxide can arise due to (i) particle size effects [38–40], (ii) stacking faults [15] (iii) interstratification of α-phase in β-nickel hydroxide [9], (iv) turbostraticity and (v) cation vacancies [39]. In our earlier work we have examined all these factors on the PXRD patterns by means of DIFFaX simulations on nickel hydroxide [40].

The PXRD pattern is a powerful tool to determine whether the sample is disordered or not. β_{bc}-nickel hydroxide display non-uniform broadening of non-($h\,k\,0$) reflections [9]. If the sample is stacking faulted, then ($0\,0\,\ell$) and ($h\,k\,0$) reflections remain unaffected while (1 0 1) and (1 0 2) reflections are considerably broadened [15]. In our earlier paper we have explicitly classified the different type of stacking faults based on the theoretical polytype nomenclature derived by Bookin and Drits [41]. Defining the stacking sequence of the ordered crystal to be AC AC AC. . ., the stacking faults can be generated by the random inclusion of other layers such as AB, BA or CA layers within the primary stacking sequence. We also determined the characteristic changes brought about in the PXRD pattern by each type of stacking fault. DIFFaX simulations show that stacking faults having the $2H_1$ and $2H_2$ motifs, obtained by the insertion of a CA layer in the AC AC AC. . . stacking sequence and exclusively affect the intensity of the (1 0 2) reflection. DIFFaX simulated powder X-ray diffraction pattern of the 1H polytype incorporating stacking faults corresponding to the $2H_2$ motifs was generated by incorporation of AB or BC layers in the AC AC AC. . . stacking sequence. The broadening of the ($h\,0\,\ell$) reflections is pronounced at the base. The peak maxima are sharp with 'wings' flaring out at the base. $3R_2$ type of stacking faults are generated by translation of layers by (1/3, 2/3, 1) with respect to each other. On the incorporation of $3R_2$ type stacking faults, a drastic broadening of the (1 0 2) reflection is observed.

The FWHM values of all reflections of nickel hydroxide samples are given in Table 5. Table 5 clearly shows that the peaks are non-uniformly broadened for ACC and SH65 nickel hydroxides. The PXRD pattern of ACC nickel hydroxide was simulated by defining the crystallite thickness to be 185 Å and 11% $3R_2$ type of stacking

Table 5
The full width at half maxima (FWHM in ±0.1° 2θ) of all the reflections in the PXRD patterns of the nickel hydroxide samples

Sample	(0 0 1)	(1 0 0)	(1 0 1)	(1 0 2)	(1 1 0)	(1 1 1)
SH65	3.16	0.7	3.0	Broad	0.6	1.1
ACC	0.6	0.3	0.9	2.1	0.5	0.6
WH65	0.27	0.24	0.3	0.38	0.35	0.39
β_{bc}-$Co_{0.05}$	3.03	0.67	2.4	Broad	0.88	1.2
β_{bc}-$Co_{0.10}$	2.58	0.62	2.2	Broad	0.7	2.0
β-$Co_{0.05}$	0.31	0.34	0.46	0.53	0.39	0.62

faults. The PXRD pattern of SH65 nickel hydroxide was simulated by incorporating 23% interstratification, 20% $3R_2$ type of stacking faults and 17% cation vacancies in β-nickel hydroxide. The goodness of the simulations was judged on the basis of the R_{wp} values (6.5 and 11% for ACC and SH65 samples) and the difference profiles of observed and the simulated PXRD patterns of ACC and SH65 nickel hydroxide samples.

Fig. 3a and b shows the PXRD patterns of 5 and 10 mol% cobalt substituted nickel hydroxide samples obtained at high pH >13 (65 °C). The PXRD patterns of cobalt substituted nickel hydroxide display non uniform broadening of non-($h\,k\,0$) reflections similar to β_{bc}-nickel hydroxide (solid lines in Fig. 2B). This indicates that substitution of cobalt in nickel hydroxide matrix does not significantly affect the crystallinity of the sample. The PXRD pattern of 5 mol% cobalt substituted β_{bc}-nickel hydroxide was simulated by defining by mixing 18% interstratification, 15% $3R_2$ type of stacking faults and 17% cation vacancies. While the PXRD pattern of 10 mol% cobalt substituted β_{bc}-nickel hydroxide was simulated by incorporation of 18% interstratification, 15% $3R_2$ type of stacking faults and 15% cation vacancies in β-nickel hydroxide (see open circles in Fig. 3a and b). This clearly indicates that the cobalt content does not drastically affect the percentage of incidence of interstratification, stacking faults and cation vacancies which contribute to the broadening of non-($h\,k\,0$) reflections in their PXRD pattern. On hydrothermal treatment of (5 mol%) cobalt β_{bc}-nickel hydroxide, all the reflections are ordered (see solid line in Fig. 3c). The simulated PXRD pattern was obtained by the incorporation restricting the crystallite size to 4590 Å and insertion of 4% $2H_2$ type of stack-

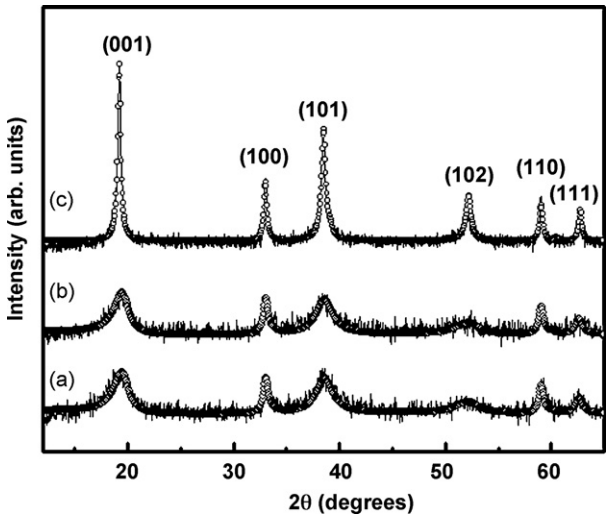

Fig. 3. Comparison of an (a) observed and the simulated PXRD patterns of 5 mol% cobalt substituted β_{bc}-nickel hydroxide, (b) 10 mol% cobalt substituted β_{bc}-nickel hydroxides obtained at 65 °C respectively and (c) observed and the simulated PXRD patterns of 5 mol% cobalt substituted β-nickel hydroxide obtained by hydrothermal treatment at 170 °C (solid line are the observed and open circles are the simulated PXRD patterns).

Table 6
Results of DIFFaX simulated PXRD patterns of different nickel hydroxide samples

Sample	Interstratification (%)	Stacking faults		Cation vacancies (%)	Crystallite size (Å) thickness disc diameter	
		$3R_2$ (%)	$2H_2$ (%)			
SH65	23	20	–	17	–	–
ACC	–	11	–	5	185	–
β-$Ni_{0.95}Co_{0.05}(OH)_2$	–	–	4	3	4590	–
β_{bc}-$Ni_{0.95}Co_{0.05}(OH)_2$	23	15	–	17	–	–
β_{bc}-$Ni_{0.90}Co_{0.10}(OH)_2$	18	15	–	17	–	–

ing faults and 3% cation vacancies (see open circles in Fig. 3c). Open circles in Fig. 3 represent the DIFFaX simulated PXRD patterns of cobalt substituted nickel hydroxide samples obtained at different experimental conditions. The results of DIFFaX simulated PXRD patterns of 5 mol%, 10 mol% cobalt substituted β_{bc}-nickel hydroxide obtained at 65 °C and 5 mol% cobalt substituted β-nickel hydroxide obtained are given in Table 6.

Transmission electron micrographs of WH65, ACC and SH65 are shown in Fig. 4. WH65 and ACC nickel hydroxide display platelet morphology (see Fig. 4a and b). Extensive regions of turbostratic disorder which is characteristic of α-nickel hydroxide could be identified in the electron micrographs of β_{bc}-nickel hydroxide, in addition to flaky platelets corresponding to the β-phase in SH65 (see Fig. 4c). In all these samples the particle size observed as agglomerates with sizes ranging from 185 to 555 Å.

3.1. Electrochemical studies

Based on the literature survey it was found that the beneficial effect of cobalt can be brought about the following mechanisms [42–44]:

(i) Cobalt addition can alter the basic structure and electrochemistry of the nickel hydroxide.
(ii) Cobalt can be used as active conductor in place of graphite being a passive conductor to provide superior conducting matrix for the active material.
(iii) On charging the nickel hydroxide electrode in presence of cobalt, it gets oxidized to $Co^{III}O(OH)$. $Co^{III}OOH$ is electrically insulating their by hinders the conductivity. On overcharging the nickel hydroxide electrode in presence of cobalt, it gets oxidized to electrically conducting $Co^{3.7+}$ state. $Co^{3.7+}$ increases the conductivity, and also undergoes reversible oxidation–reduction. The redox reaction also contributes to the number of electron exchange thereby misleading it as a factor increasing the electrochemical performance of nickel hydroxide electrode.
(iv) *Formation of Ni^{II}–Co^{III} layered double hydroxide*: During charge discharge process of a nickel hydroxide electrode, cobalt gets oxidized to Co^{3+} state. On discharge it does not get reduced. At this stage the composition of the sample changes from $Ni_xCo_{1-x}(OH)_2$ to $Ni_x^{2+}Co_{1-x}^{3+}(OH)_{2-x}(CO_3)_{x/n}\cdot H_2O$. Earlier co-workers from our laboratory have shown that layered double hydroxide such as $Ni_{0.8}Al_{0.2}(OH)_{2-x}(CO_3)_{x/n}\cdot xH_2O$ exchanges 1.7e/Ni atom [45,46]. Thus Ni^{II}–Co^{III} layered double hydroxide delivers >1e exchange misleading it to the effect of cobalt contribution in β_{bc}-nickel hydroxide [22,23].

Our objectives in this study are two-fold:

(i) To partially replace the passive conducting material (graphite) by an electronic conducting one (cobalt powder) during the electrode fabrication and monitor the electrochemical activities of different nickel hydroxide samples. If the electrochemical activity was dependent on the conductivity alone then poorly performing electrodes should show dramatic improvement in their electrochemical activity.
(ii) If cobalt can affect the crystal structure and the electrochemical activity of nickel hydroxide, then we were interested to prepare chemically modified nickel hydroxide matrix by coprecipitation of cobalt as Co^{2+} in presence of Ni^{2+} ions.

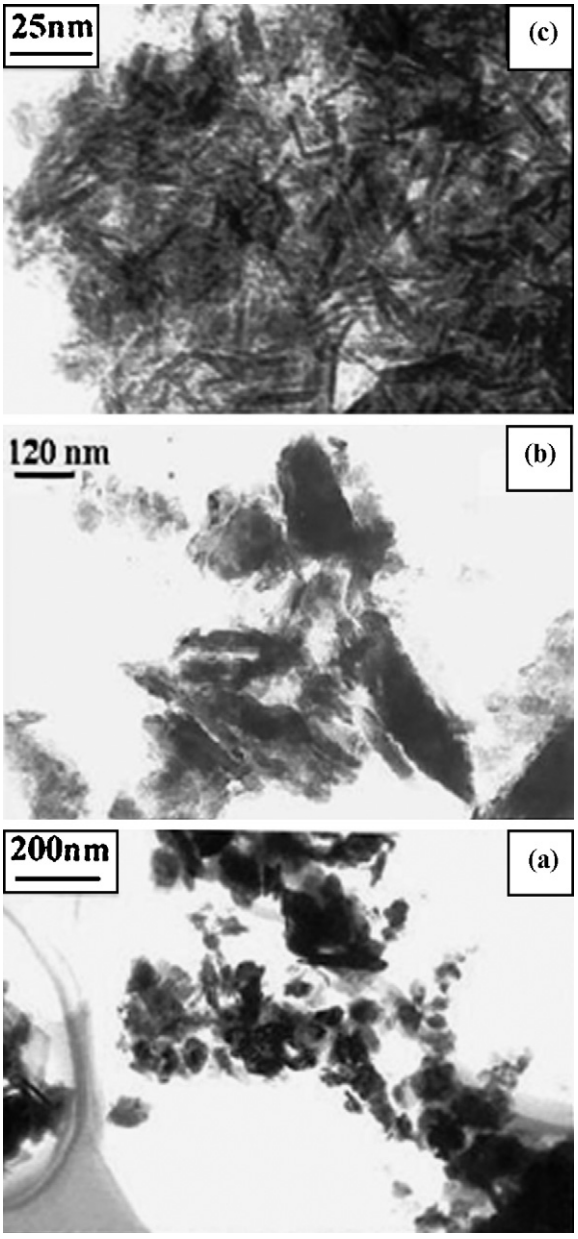

Fig. 4. TEM images of (a) WH65 nickel hydroxide, (b) ACC nickel hydroxide and (c) SH65 nickel hydroxide.

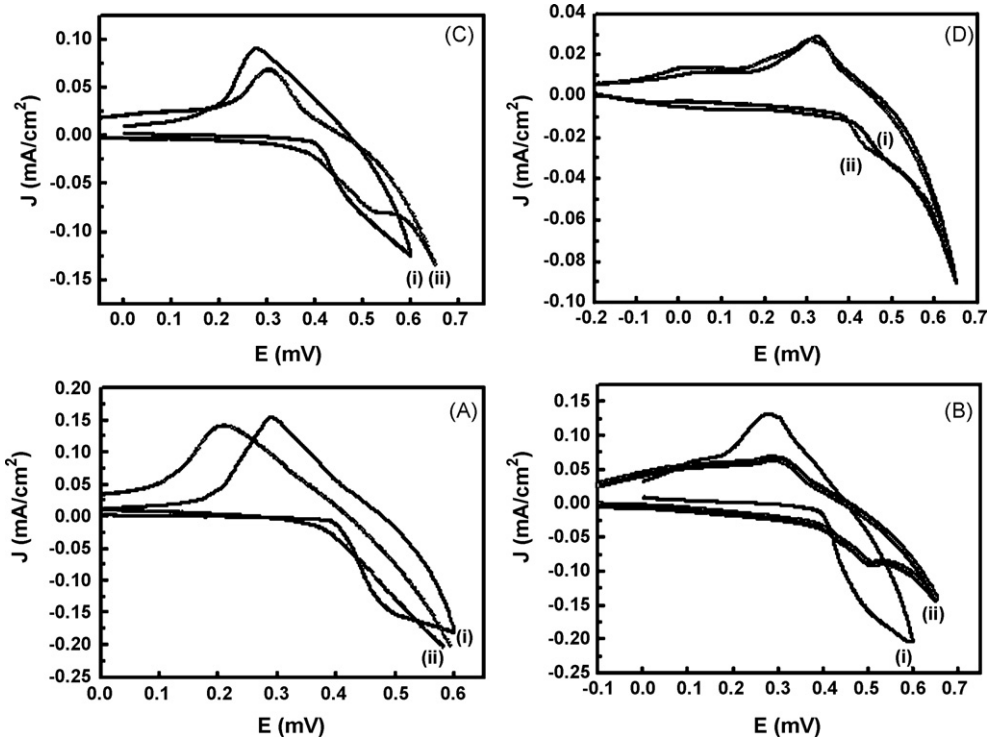

Fig. 5. Cyclic voltammograms of (Ai) WH65 nickel hydroxide (Aii) WH65 nickel hydroxide in presence of cobalt (Bi) ACC nickel hydroxide (Bii) ACC nickel hydroxide in presence of cobalt (Ci) SH65 nickel hydroxide (Cii) SH65 nickel hydroxide in presence of cobalt and (Di) 5 mol% cobalt substituted β_{bc}-nickel hydroxide (Dii) 5 mol% cobalt substituted β-nickel hydroxide obtained by hydrothermal treatment at 170 °C.

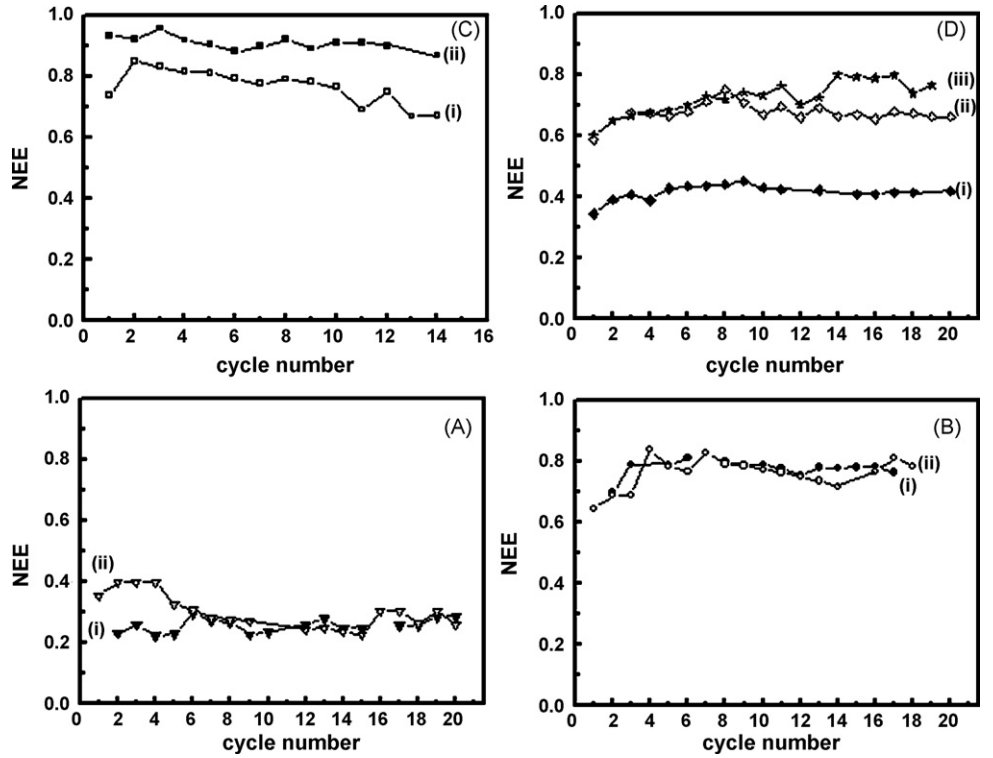

Fig. 6. Cycle life data of (Ai) WH65 nickel hydroxide (Aii) WH65 nickel hydroxide in presence of cobalt (Bi) ACC nickel hydroxide (Bii) ACC nickel hydroxide in presence of cobalt (Ci) SH65 nickel hydroxide (Cii) SH65 nickel hydroxide in presence of cobalt and (Di) 5 mol% cobalt substituted β-nickel hydroxide obtained by hydrothermal treatment at 170 °C (Dii) 5 mol% cobalt substituted β_{bc}-nickel hydroxide (Diii) 10 mol% cobalt substituted β_{bc}-nickel hydroxide.

Table 7
The results of cyclic voltammograms of the nickel hydroxide samples with its reversible discharge capacities based on the galvanostatic charge discharge studies

Sample	Potentials (mV)		Specific capacity (±10 mAh g^{-1})
	Oxidation	Reduction	
WH65	212	Broad peak	70
WH65 + Co	290	Broad peak at 492	80
ACC	282	494	209
ACC + Co	295	505	207
SH65	276	490	250
SH65 + Co	303	522	220
β-$Ni_{0.95}Co_{0.05}(OH)_2$	325	433	115
β_{bc}-$Ni_{0.95}Co_{0.05}(OH)_2$	322	489	195
β_{bc}-$Ni_{0.90}Co_{0.10}(OH)_2$	–	–	209

Fig. 5 shows the cyclic voltammograms of nickel hydroxide samples in presence of cobalt addition and also chemically substituted nickel hydroxides. All the nickel hydroxide samples display oxidation and reduction peaks (see Table 7) (see solid lines in Fig. 5A–D). When a part of graphite was replaced by cobalt during electrode fabrication, we observed positive shifts in oxidation and reduction potentials (see Table 7). Cyclic voltammograms are the represented profiles of various nickel hydroxide samples. Extensive charge–discharge studies were carried out in order to monitor the role of cobalt in various nickel hydroxide samples. Fig. 6Ai, Bi and Ci shows the cycle life data of WH65, ACC and SH65 nickel hydroxide electrodes. Electrodes comprising ACC and SH65 nickel hydroxide samples exchange 0.8–0.9e/Ni. This is in sharp contrast to the electrochemical performance of WH65 nickel hydroxide electrodes with 0.3e/Ni (see Fig. 6Ai). In Table 7 is given the specific discharge capacities of all the nickel hydroxide samples. The good electrochemical activities of ACC and SH65 nickel hydroxide samples are associated to the presence of structural disorders.

We thought that it would be interesting to partially replace a 50 wt% of graphite with 50 wt% cobalt and expected a dramatic improvement in the electrochemical performance of WH65 nickel hydroxide. We also prepared cobalt substituted crystalline phase of β-nickel hydroxide on hydrothermal treatment at 170 °C and examined the electrochemical behaviour. If conductivity is the sole determining factor then we should expect a dramatic improvement in the electrochemical performance of WH65 nickel hydroxide and β-$Ni_{0.95}Co_{0.05}(OH)_2$ due to the presence of cobalt. Fig. 6Di shows the electrochemical performance of WH65 with cobalt addition in place of graphite and crystalline β-$Ni_{0.95}Co_{0.05}(OH)_2$. There was no improvement in the electrochemical activities of both the samples.

We also partially replaced 50 wt% of graphite with 50 wt% cobalt in ACC and SH65 nickel hydroxide electrodes which already exchanges 0.8–0.9e/Ni and expected further improvement. Fig. 6Bii and Cii shows the cycle life data of ACC and SH65 with cobalt addition. It is clearly evident from Fig. 6 that cobalt does not affect the inherent nature of the redox reaction and does not contribute to the enhancement in the electrochemical performance.

The PXRD patterns of cobalt substituted β_{bc}-phases of nickel hydroxide is similar to that of β_{bc}-nickel hydroxide (SH65). We expected that cobalt as a substitute for nickel could still contribute to the electrochemical property of the material (see Fig. 3). Fig. 6Dii and Diii shows the cycle life data of the cobalt substituted β_{bc}-nickel hydroxide electrodes [β_{bc}-$Ni_{0.95}Co_{0.05}(OH)_2$; β_{bc}-$Ni_{0.90}Co_{0.10}(OH)_2$]. The results show that these electrodes exchange 0.65–0.7e/Ni, which is less than that of β_{bc}-nickel hydroxide. This clearly indicates that incorporation of cobalt into the nickel hydroxide matrix does not increase the electrochemical performance of β_{bc}-nickel hydroxide electrode. In Fig. 7A–D are shown the 20th cycle discharge curves of WH65, ACC, SH65 and with partial replacement of graphite with cobalt, cobalt substituted nickel hydroxides [β-$Ni_{0.95}Co_{0.05}(OH)_2$; β_{bc}-$Ni_{0.95}Co_{0.05}(OH)_2$].

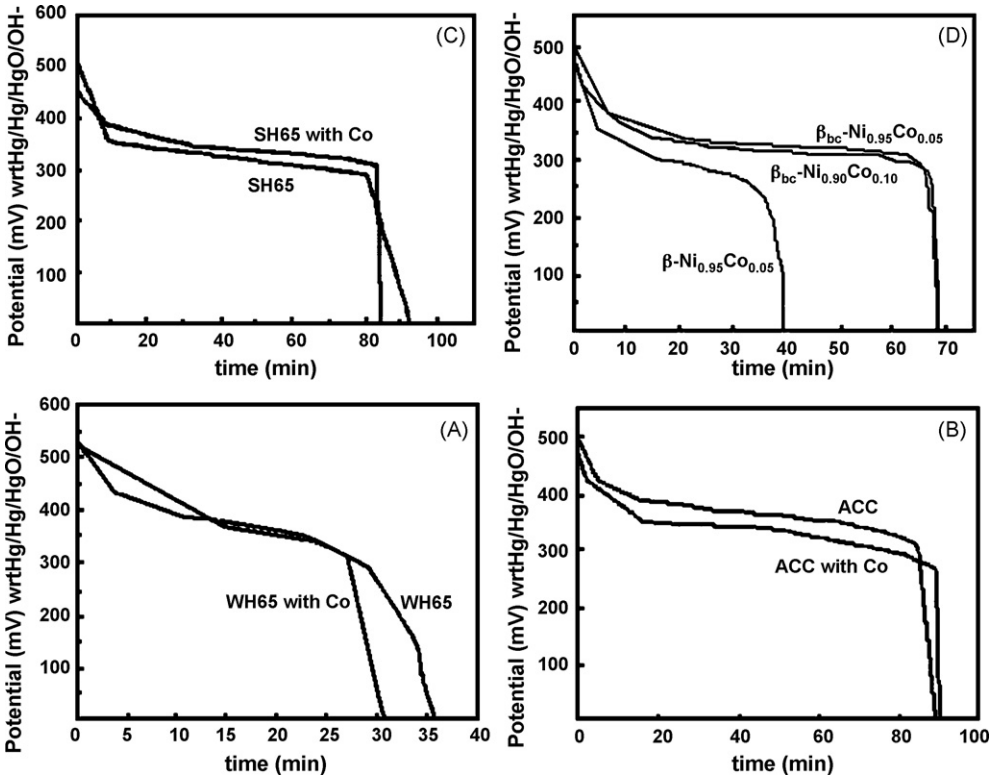

Fig. 7. 20th cycle discharge curves of (A) WH65, (B) ACC, (C) SH65 without and with cobalt additive and (D) cobalt substituted nickel hydroxides.

Any variation in the precipitation conditions yields nickel hydroxide with sub-optimal quality which adversely affect the reversible charge storage capacity such as WH65. The electrochemical activity cannot be improved by mere substitution of cobalt either physically or chemically. The better electrochemical performance in the nickel hydroxide is achieved by careful control during the precipitation which can incorporate disorder. The decrease in conductivity of cobalt doped β_{bc}-nickel hydroxide compared to β_{bc}-nickel hydroxide was also been reported by Deabate et al. [7].

ACC nickel hydroxide delivers better electrochemical activity due to the presence of structural disorder compared to WH65 nickel hydroxide. The SH65 nickel hydroxide and the cobalt substituted β_{bc}-nickel hydroxide samples also shows reasonable electrochemical activities due to the presence of structural disorders in the crystal. Cobalt will merely act as a conducting material in the electrodes at 25–30 °C. The beneficial effects of cobalt addition are indeed not due to the presence of cobalt, but actually due to the existence of structural disorder in the crystal structure of nickel hydroxide.

4. Conclusion

We report for the first time, that the addition of cobalt metal in place of graphite during the electrode fabrication of pasted electrodes or substitution of cobalt within the nickel hydroxide matrix during precipitation does not enhance the electrochemical activity. Addition of expensive cobalt as additive or as a substituent into nickel hydroxide is not required to achieve better electrochemical activity. Structural disorder is the sole determining factor for the optimum performance in nickel hydroxide at 25–30 °C.

Acknowledgements

TNR thanks Council of Scientific and Industrial Research (CSIR) Government of India for the awards of Research Associate Fellowship (RA), Senior Research Fellowship (NET) and PVK is grateful to the Department of Science and Technology, Government of India (GOI) for financial support and is a recipient of Ramanna Fellowship from DST. The authors thank Solid State and Structural Chemistry Unit, Indian Institute of Science for providing powder X-ray diffraction facilities.

References

[1] S.R. Ovshinsky, J. Non-cryst. Solids 32 (1979) 17.
[2] A.-C. Gaillot, V.A. Drits, A. Plancon, B. Lanson, Chem. Mater. 16 (2004) 1890.
[3] L. Kienle, V. Duppel, A. Simon, M. Schlosser, O. Jarchow, J. Solid State Chem. 177 (2004) 6.
[4] S.U. Falk, A.J. Salkind, Alkaline Storage Batteries, Wiley, New York, 1969.
[5] H. Bode, K. Dehmelt, J. Witte, Electrochim. Acta 11 (1966) 1079.
[6] P. Oliva, J. Leonardi, J.F. Laurent, C. Delmas, J.J. Braconnier, M. Figlarz, F. Fievet, A. De Guibert, J. Power Sources 8 (1982) 229.
[7] S. Deabate, F. Henn, S. Devautour, J.C. Giuntini, J. Electrochem. Soc. 150 (2003) 23.
[8] J. McBreen, in: R.E. White, J.O'M. Bokris, B.E. Conway (Eds.), Modern Aspects of Electrochemistry, No. 21, Plenum Press, NY, 1990.
[9] T.N. Ramesh, R.S. Jayashree, P.V. Kamath, S. Rodrigues, A.K. Shukla, J. Power Sources 104 (2001) 295.
[10] C. Faure, C. Delmas, C. Fouassier, J. Power Sources 35 (1991) 279.
[11] A. Audemer, A. Delahaye-Vidal, R. Farhi, N. Sac-Epee, J.-M. Tarascon, J. Power Sources 57 (1995) 137.
[12] R.S. Jayashree, P.V. Kamath, G.N. Subbanna, J. Electrochem. Soc. 147 (2000) 2029.
[13] L. Hui, D. Yunchang, Y. Jiongliang, W. Zeyun, J. Power Sources 57 (1995) 137.
[14] T.N. Ramesh, R.S. Jayashree, P.V. Kamath, J. Electrochem. Soc. 150 (2003) 520.
[15] C. Delmas, C. Tessier, J. Mater. Chem. 7 (1997) 602.
[16] T.N. Ramesh, P.V. Kamath, C. Shivakumara, J. Electrochem. Soc. 152 (2005) 806.
[17] A. Yuan, S. Cheng, J. Zhang, C. Cao, J. Power Sources 77 (1999) 178.
[18] C. Sigala, A. Verbaere, J.L. Mansot, D. Guyomard, Y. Piffard, M. Tournoux, J. Solid State Chem. 132 (1997) 372.
[19] X. Wang, J. Yan, H. Yuan, Z. Zhou, D. Song, Y. Zhang, L. Zhu, J. Power Sources 72 (1998) 221.
[20] M. Oshitani, H. Yufu, K. Takashima, S. Tsuji, Y. Matasumaru, J. Electrochem. Soc. 136 (1989) 1590.
[21] V. Pralog, A. Delahaye-Vidal, B. Beaudoin, B. Gerand, J.B. Leriche, J.-M. Tarascon, J. Electrochem. Soc. 147 (2000) 1306.
[22] R.D. Armstrong, G.W.D. Briggs, E.A. Charles, J. Appl. Electrochem. 18 (1988) 215.
[23] M. Oshitani, T. Takayama, K. Takashima, S. Tsuji, J. Appl. Electrochem. 16 (1986) 403.
[24] L. Jun, L. Rong, S. Hang, J. Power Sources 79 (1999) 86.
[25] R.S. Jayashree, P.V. Kamath, J. Electrochem. Soc. 149 (2002) 761.
[26] A.B. Yuan, S.A. Chang, J.Q. Zand, C.A. Cao, J. Power Sources 77 (1999) 178.
[27] A.B. Yuan, N.X. Xu, J. Appl. Electrochem. 31 (2001) 245.
[28] A.K. Sood, J. Appl. Electrochem. 16 (1986) 274.
[29] R. Sjovall, J. Power Sources 90 (2000) 153.
[30] A. Audemer, A. Delahaye-Vidal, R. Farhi, N. Sac-Epee, J.-M. Tarascon, J. Electrochem. Soc. 144 (1997) 2614.
[31] J. Chen, D.H. Bradhurst, S.X. Dou, H.K. Liu, J. Electrochem. Soc. 146 (1999) 3606.
[32] K. Watanabe, N. Kumagai, J. Power Sources 76 (1998) 167.
[33] C. Fierro, A. Zallen, J. Koch, M.A. Fetcenko, J. Electrochem. Soc. 153 (2006) 492.
[34] C. Greaves, M.A. Thomas, Acta Crystallogr. B 42 (1986) 51.
[35] M.M.J. Treacy, J.M. Newsam, M.W. Deem, Proc. R. Soc. Lond. A 433 (1991) 499.
[36] T.N. Ramesh, P.V. Kamath, C. Shivakumara, Acta Crystallogr. B 62 (2006) 530.
[37] R.A. Young, The Rietveld Method, IUCr, Oxford University Press, New York, 1993.
[38] M.C. Bernard, R. Cortes, M. Keddam, H. Takenouti, P. Bernard, S. Senyarich, J. Power Sources 63 (1996) 247.
[39] B.C. Cornilsen, P.J. Karjala, P.L. Loyselle, J. Power Sources 22 (1988) 351.
[40] T.N. Ramesh, R.S. Jayashree, P.V. Kamath, Clays Clay Miner. 51 (2003) 570.
[41] A.S. Bookin, V.A. Drits, Clays Clay Miner. 41 (1993) 551.
[42] V. Pralong, A. Delahaye-Vidal, B. Beaudoin, B. Gerand, J.-M. Tarascon, J. Mater. Chem. 9 (1999) 955.
[43] M. Butel, L. Gautier, C. Delmas, Solid State Ionics 122 (1999) 271.
[44] P. Bernard, J. Electrochem. Soc. 145 (1998) 456.
[45] J.J. Braconnier, C. Delmas, C. Foussier, M. Figlarz, B. Beaudouin, P. Hagenmuller, Rev. Chim. Miner. 21 (1984) 496.
[46] P.V. Kamath, M. Dixit, L. Indira, A.K. Shukla, V.G. Kumar, N. Munichandraiah, J. Electrochem. Soc. 141 (1994) 2956.